Hydrogen production from methane using an RF plasma source in total nonambipolar flow

2012 Plasma Sources Sci. Technol. 21 015007

(http://iopscience.iop.org/0963-0252/21/1/015007)

Plasma Sources Sci. Technol. **21** (2012) 015007 (8pp) doi:10.1088/0963-0252/21/1/015007

Hydrogen production from methane using an RF plasma source in total nonambipolar flow

Benjamin W Longmier[1], Alec D Gallimore[2] and Noah Hershkowitz[3]

[1] University of Houston, 617 Science and Research I, Houston, TX 77204-5005, USA
[2] University of Michigan, 3037 FXB, 1320 Beal Avenue, Ann Arbor, MI, USA
[3] University of Wisconsin, 1500 Engineering Dr, Madison, WI, USA

E-mail: blongmier@uh.edu

Received 28 August 2011, in final form 22 December 2011
Published 31 January 2012
Online at stacks.iop.org/PSST/21/015007

Abstract
A radio-frequency (RF) helicon plasma reaction chamber (HPRC) is developed and used to decompose methane gas into high-purity hydrogen gas and solid carbon in the form of graphite. A single-turn ($m = 0$) helicon antenna, operated at 13.56 MHz, and a 100 G dipole magnetic field are used to excite a helicon mode in a nonthermal plasma, creating plasma densities exceeding 10^{13} cm^{-3} using 8–20 SCCM methane gas at up to 1300 W of RF power. The HPRC device takes advantage of a uniform large amplitude electron sheath across the exit aperture. At this aperture, all of the incident electron flux from the plasma is extracted and all ions are reflected back into the source. In this way, only neutrals and electrons are allowed out of the reaction chamber, enhancing the breakdown of methane into deposited carbon and hydrogen gas that escapes. A methane decomposition percentage of $99.99 \pm 0.06\%$ is demonstrated using 1300 W of RF power and a methane gas flow rate of 8 SCCM. A total nonambipolar flow of particles maximizes the recirculation of ions, and leads to the very high degree of molecular decomposition achieved in this proof-of-concept device. The HPRC in its present proof-of-concept form requires 37× more energy per kg of H_2 produced, compared with steam-methane reformation, though this energy comparison does not include the energy required to sequester the emitted CO_2 during the steam–methane reformation cycle.

(Some figures may appear in colour only in the online journal)

1. Introduction

Should countries move to reduce carbon dioxide emissions as part of the commitment to greenhouse gas reduction, the percentage of hydrogen-containing fuels such as natural gas and methane hydrates in the global economy's total energy budget could increase. Increasing emphasis has also been put on automobile manufacturers to produce low or 'zero' emission vehicles. Proposed next-generation vehicles with large travel ranges could likely take advantage of fuel cells that require hydrogen gas to generate electricity. As a result, an increase in efficient hydrogen production will be a necessity, and new energy-efficient methods for hydrogen production and extraction must be realized on both centralized and distributed geographic scales.

The current method for hydrogen extraction from methane involves combining water vapor and methane in a high-temperature reaction chamber, where carbon monoxide (or carbon dioxide) and hydrogen gases are extracted. Currently, this process involves a large amount of heating in order to raise the temperature of the methane–steam mixture to a point where a large degree of molecular dissociation occurs [1]. An unintended consequence of this reformation reaction is that a large amount of carbon dioxide is released directly into the atmosphere, typically ~ 0.3 mol of CO_2 for 1 mol of H_2 [1].

A second-stage plasma source, sometimes referred to as a catalytic plasma source, can reduce the energy required to dissociate hydrogen from various hydrogen-containing compounds such as methane gas [2–7]. However, these existing plasma-aided hydrogen extraction techniques do not

take advantage of the electrode-less nature and high degree of ionization that a helicon plasma source provides. It is believed that techniques that currently use a plasma second-stage (or some type of plasma catalysis) can be improved and could even replace existing methane-gas–steam hydrogen production methods if the energy efficiency of such plasma devices [8] comes close to that of steam–methane reformation plus CO_2 energy sequestering costs.

This paper identifies some of the key aspects of utilizing high-density radio-frequency (RF) plasma sources such as a helicon source to provide a very high degree of molecular dissociation and ionization in order to isolate hydrogen gas from methane gas. Alhough this paper is limited in scope to a set of proof-of-concept experiments performed using methane gas, the method employed here is applicable to a large variety of decomposition applications. In principle, any hydrogen-containing molecule (e.g. water) would serve the same purpose as methane in the production of hydrogen gas.

The ideas presented here take advantage of previous work on a helicon plasma source focused on producing an electron-emitting device for use in high-power (>50 kW) ion propulsion systems for space vehicles [8–11]. Within the helicon plasma source, a single-turn ($m = 0$) helicon antenna excites a helicon mode [12] in either an argon or xenon plasma, and electrons are extracted through an electron sheath that exists in the form of an electrostatic lens at the exit aperture of the device. The ions that are produced in the system are repelled by this strong electron sheath and hence are prevented from leaving the system through the aperture. Ions are lost only through recombination at the interior walls of the device through an ion sheath that forms at the cylindrical graphite electrode. Once neutralized, the newly formed neutral either leaves the system through the exit aperture or becomes re-ionized and participates in another recombination event at the ion sheath. On average, a neutral particle injected into the system participates in 130 or more ionization and recombination cycles before escaping through the exit aperture. If the ratio of the electron sheath area to the ion sheath area is kept at $\sqrt{2m_i/\pi m_e}$ (see equation (3)), the flow of electrons and ions becomes nonambipolar, and thus a large flux of electrons can be extracted from the plasma with the most efficient use of input gas. It is this same principle that is taken advantage of in the decomposition of methane, and the reason that a very high degree of dissociation can be achieved with this particular proof-of-concept device.

2. Helicon plasma reaction chamber and supporting hardware

The helicon plasma reaction chamber (HPRC), electromagnet, residual gas analyzer (RGA), and supporting vacuum equipment used in the production of hydrogen gas and solid carbon from an input methane gas are described below.

2.1. Helicon plasma reaction chamber

The HPRC contains a 21 cm long hollow graphite cylinder with an inner diameter of 5.6 cm and an outer diameter of 7 cm that is located coaxially within a quartz tube. A graphite disc that is inside the graphite cylinder is mounted on a movable shaft to alter the volume that could be occupied by the plasma. The graphite cylinder serves as the ion collection surface and is biased at −60 V with respect to an extraction ring (figure 1). This ion collection cylinder is a radial boundary for the plasma and acts as a location for the formation of an ion sheath that both collects ions and reduces electron leaks to the chamber walls. The ion collection cylinder has eight axial slits that allow the time-varying magnetic fields into the plasma but limit the penetration of the time-varying electric fields [13], effectively serving as a Faraday shield for the plasma within the reaction chamber. The eight Faraday shield slits are 0.1 cm wide, 20 cm long, and are spaced at 45° intervals around the circumference of the graphite cylinder (figure 1(*b*)). The use of a Faraday shield significantly reduces the amplitude of plasma potential fluctuations [14]. The electron extraction ring is an electrically grounded graphite ring with a 1.25 cm diameter aperture that sits inside of an insulating boron nitride end cap that functions as a gas limiter. This grounded electron extraction ring, combined with the magnetic field, creates an electron sheath that is uniform across the ring. The uniform electron sheath limits the ion flow, and gives a potential reference for the plasma with respect to the extraction ring. The RF antenna is formed from a single turn of 0.63 cm diameter water-cooled copper tubing and operates at power levels up to 1300 W at an RF frequency of 13.56 MHz. The magnet coil geometry and resulting magnetic field are discussed below.

2.2. Magnetic field geometry

An electromagnet coil generates a steady-state dipole magnetic field within the plasma reaction chamber (figure 2). The strength of the magnetic field at the location of the electron extraction ring is 100 G. Although not used for this set of methane experiments, a set of permanent axially magnetized ferrite magnets can be used to produce a similar steady-state magnetic field with a fixed intensity [14, 15]. Either magnet arrangement produces a moderately strong magnetic field in the region of the RF antenna and the electron extraction ring. When present, the magnetic field ensures that the electrons follow the field lines that pass through the exit region of the electron extraction ring, and that fewer electrons are lost to the interior walls of the extraction ring. The presence of the magnetic field creates a uniform plasma potential across the surface of the extraction aperture, ensuring that all ions are reflected from the electron sheath [8, 16]. The magnetic field also allows for the single-turn ($m = 0$) helicon antenna to excite a helicon mode within the plasma, which acts to increase the plasma density by a factor of ∼10 compared with operation in an inductive mode, leading to an increased ability to decompose methane and confine partially decomposed products.

2.3. Residual gas analyzer

A Stanford Research Systems RGA100 RGA is used to detect the presence and concentration of methane, hydrogen and other trace gases in the main section of the vacuum chamber, downstream of the reaction chamber. The RGA100 unit is

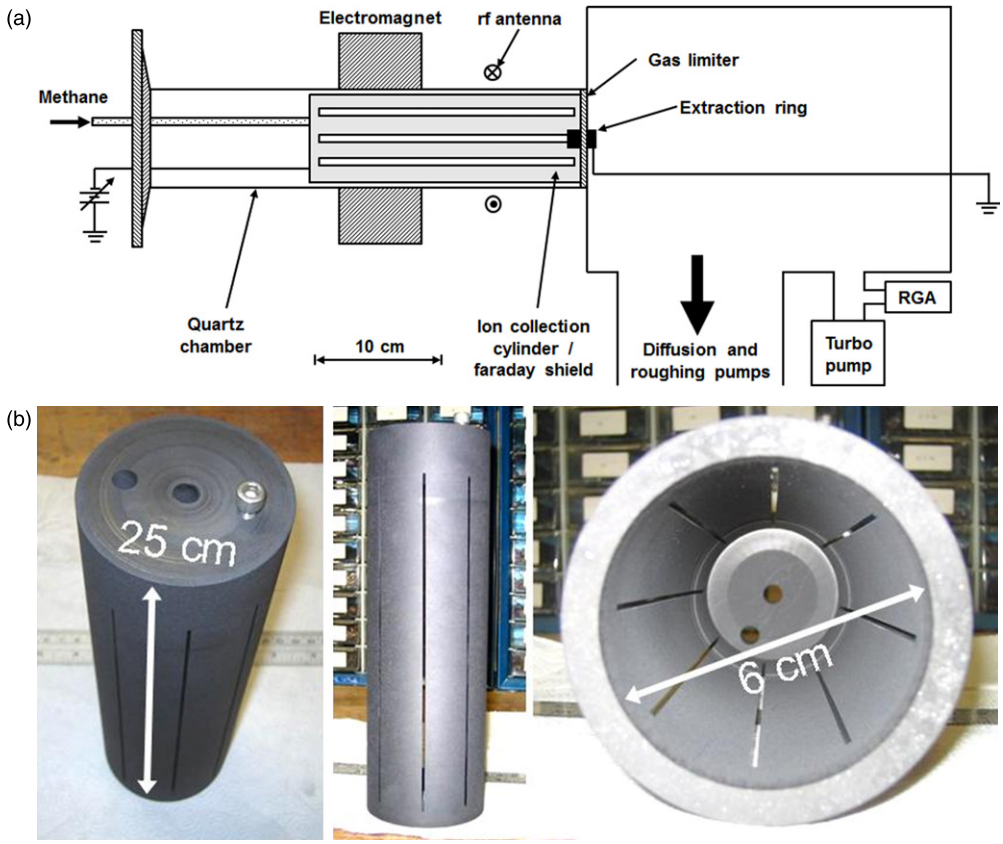

Figure 1. (*a*) Schematic of the HPRC, supporting vacuum hardware and differentially pumped RGA. (*b*) Photograph of the HPRC ion collection cylinder/Faraday shield.

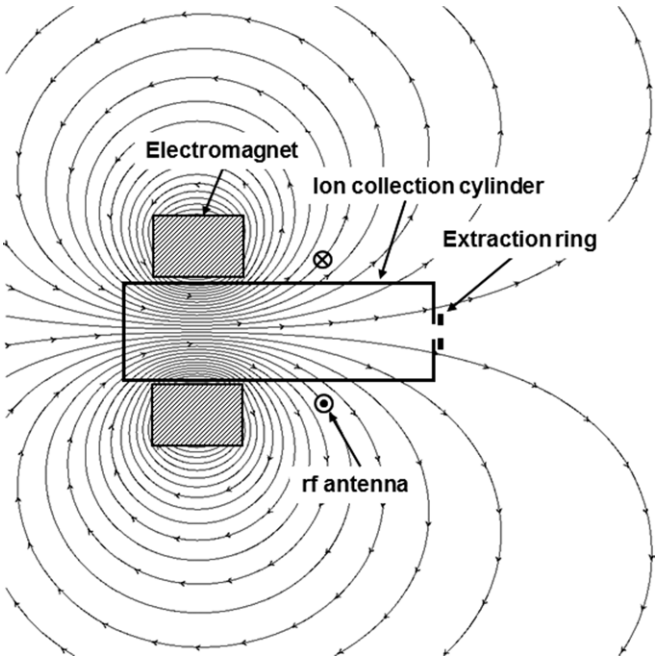

Figure 2. Simulation of the dipole magnetic field lines produced by the electromagnet. The ion collection cylinder, RF antenna and electron extraction ring are superimposed. The field strength at the extraction ring is 100 G.

capable of detecting compounds with an atomic mass unit (amu) between 1 and 100, with a resolution of 0.1 amu and a partial pressure detection level of 10^{-14} Torr. Because relatively large flow rates are used within the reaction chamber and vacuum chamber, the RGA is differentially pumped by a 100 l s^{-1} turbopump in order to ensure that the filament of the RGA does not experience an absolute pressure above 10^{-4} Torr. The RGA inherently breaks down a small fraction of the methane gas (and other compounds) into hydrogen as a function of the methane partial pressure at the RGA filament. This baseline breakdown of CH_4 and residual H_2O into H_2 is subtracted from all data reported in the paper.

2.4. Vacuum chamber and pumps

The components of the reaction chamber are attached to a 25 cm long by 20 cm diameter vacuum chamber. The vacuum chamber houses a diffusion pump that is backed by a roughing pump, and creates a base vacuum pressure of 5×10^{-7} Torr. With a standard operating methane gas flow rate of 8 SCCM, the chamber pressure external to the HPRC is 1×10^{-4} Torr. At 8 SCCM, the pressure inside the HPRC is 2×10^{-3} Torr.

3. Hydrogen production from methane

The flow rate of input methane gas was varied from 8 to 20 SCCM in an effort to characterize the purity of hydrogen gas that was produced. At a fixed RF power level of 1300 W,

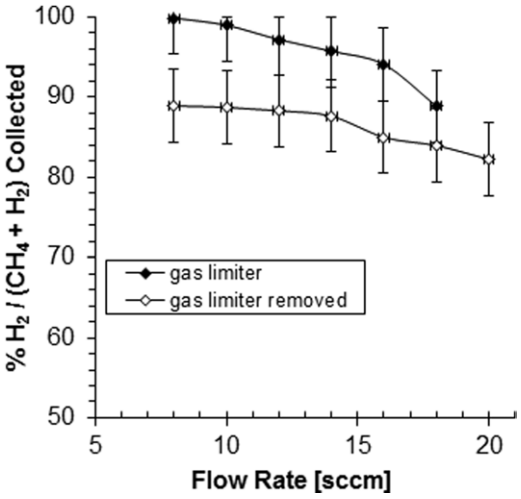

Figure 3. The percentage of hydrogen gas produced from methane gas as a function of the input methane gas flow rate with (black diamonds) and without (white diamonds) a gas limiter at the exit of the reaction chamber. Applied RF power is 1300 W.

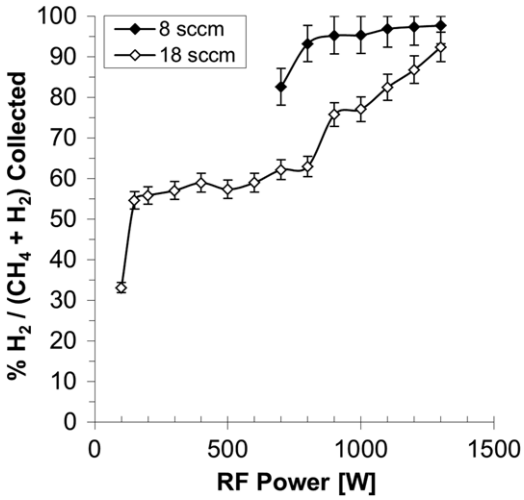

Figure 4. The percentage of hydrogen gas produced from methane gas as a function of the applied RF power level for 8 SCCM of input methane gas (black diamonds) and for 18 SCCM of input methane gas (white diamonds).

and a fixed magnetic field strength of 100 G, the hydrogen production factor was found as a function of the input methane gas flow rate. The hydrogen production factor, α, is defined as the percentage of the hydrogen partial pressure to the sum of the hydrogen and methane partial pressures downstream of the HPRC device,

$$\alpha = \frac{p_{H_2}}{p_{CH_4} + p_{H_2}} \tag{1}$$

and is presented in figure 3 as black diamonds as a function of input methane gas flow rate.

As the input methane gas flow rate is reduced down to 8 SCCM, α in the downstream vacuum collection chamber reaches 95% to 100% (figure 1, black diamonds). Although not graphed, another way to look at the effectiveness of the reaction chamber to break apart the methane gas is to compare the ratio of methane partial pressures before and after the RF power is turned on within the reaction chamber to form a plasma. At an RF power level of 1300 W and a magnetic field strength of 100 G, the percentage of methane gas that is decomposed is found to be 99.99 ± 0.06%. The methane decomposition percentage is found by comparing the measured methane partial pressure with the RF turned off (i.e. no plasma) versus the RF turned on (i.e. with plasma), and is expressed as $100(1 - p_{CH_4 no\_RF}/p_{CH_4 RF})$. As the input methane gas flow rate increases up to 20 SCCM, the fraction of hydrogen gas produced decreases to 89 ± 4% of the outflowing gas. In an effort to gauge the effectiveness of the total nonambipolar process, the gas limiter (figure 1) was removed from the system and the experiments were repeated, shown as white diamonds in figure 3 as a function of the input methane gas flow rate. With the gas limiter removed, the percentage of outflowing hydrogen gas from the HPRC was significantly reduced at all flow rates, making the system much less efficient at breaking apart the methane gas and forming hydrogen.

The HPRC was intentionally operated in a helicon mode, an inductive mode, and a capacitive mode in order to investigate the effectiveness of each RF coupling mode at decomposing the input methane gas into hydrogen gas. The HPRC was operated at two flow rates, 8 and 18 SCCM, a fixed magnetic field strength of 100 G, and over a range of RF power levels from 0 to 1300 W (figure 4).

As seen in figure 4, the HPRC operating at a methane gas flow rate of 18 SCCM goes through all three of the described plasma coupling modes, from a capacitive mode to an inductive mode between 100 and 150 W, and from an inductive mode to a helicon mode between 800 and 900 W. The data at an input methane flow rate of 8 SCCM only show a transition from an inductive mode to a helicon mode between 700 and 800 W, as RF power levels below 700 W are unable to sustain the discharge at a flow rate of 8 SCCM. The percentage of hydrogen produced, α, in the 8 SCCM data ranges from 83 ± 4% to 98 ± 4%, and 33 ± 4% to 92 ± 4% for the 18 SCCM flow rate. If the RF generator used in the setup had the ability to go to higher power levels, it is expected that a higher percentage of hydrogen could have been produced, particularly in the 18 SCCM data, and at much higher input methane gas flow rates.

The energy cost, E_{H_2}, for the production of hydrogen gas was found by dividing the applied RF power by the H_2 particle flow rate produced by the HPRC,

$$E_{H_2} = \frac{P_{RF}}{2\dot{m}_{CH_4}\left(p_{H_2}/(p_{CH_4} + p_{H_2})\right)}, \tag{2}$$

where P_{RF} is the RF power, $\dot{m}_{CH_4}$ is the input methane gas flow rate, p_{H_2} is the partial pressure of hydrogen gas in the collection chamber and p_{CH_4} is the partial pressure of methane gas in the collection chamber.

This energy cost is graphed as a function of the input methane gas flow rate in figure 5 as electron volts (eV) per H_2 molecule collected. Figure 5 presents two data sets, one where the HPRC uses the gas limiter (black diamonds) and one where the gas limiter is removed from the system (white diamonds).

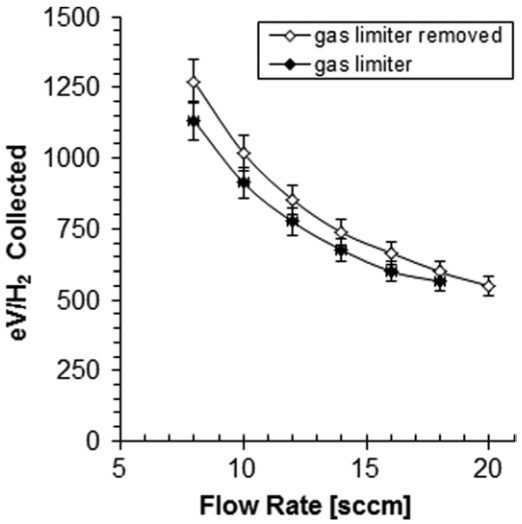

Figure 5. The energy required (in eV) per H_2 molecule produced as a function of the input methane gas flow rate for a fixed RF power level of 1300 W with (black diamonds) and without (white diamonds) a gas limiter at the exit of the reaction chamber.

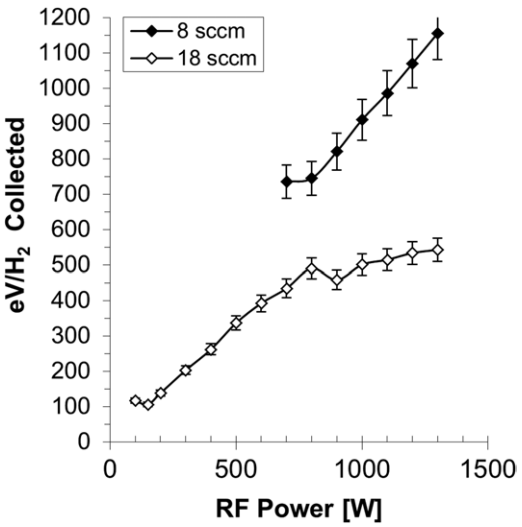

Figure 6. The energy required (in eV) per H_2 molecule produced as a function of the applied RF power level for 8 SCCM of input methane gas (black diamonds) and for 18 SCCM of input methane gas (white diamonds).

Note that the required energy is reduced by approximately a factor of 2, as the flow rate is increased from 8 to 20 SCCM. The power consumed by the electromagnet, dc power supplies and pumps was not included in this simplified estimate.

The energy cost is also graphed as a function of the applied RF power to the HPRC (figure 6). A flow rate of 8 SCCM (black diamonds) yields an energy cost between 735 and 1155 eV/H_2 between 700 and 1300 W of RF power. However, with an increased input methane gas flow rate of 18 SCCM, the data show a hydrogen production energy cost of 106 to 543 eV/H_2 for RF power levels between 100 and 1300 W.

4. Discussion

The proof-of-concept HPRC was able to produce a high-purity stream of hydrogen gas from input methane gas with the use of RF power, an externally applied steady-state magnetic field, an applied dc electric current with a bias of −60 V with respect to an extraction ring and a carefully designed reaction chamber that induced total nonambipolar flow of the ions and electrons. The only by-products from the reaction chamber were high-purity hydrogen gas, carbon in the form of solid graphite and heat rejected from the system. The HPRC is unique compared with existing steam reformation technology in that it is a small table-top sized device, has the potential to be scaled up, and does not require expensive catalyst materials or a factory scale infrastructure to operate.

A gas limiter, shown in figure 1, was used to effectively increase the neutral pressure within the reaction chamber, and limited ion and neutral flow out of the chamber except through a small aperture where a large amplitude electron sheath existed. The gas limiter was effective at increasing the hydrogen production and energy efficiency of the HPRC without an increase in methane gas flow rate or applied RF power (figure 3). The role of the electron sheath is addressed in more detail in section 4.1.

The data from figure 4 indicate plasma coupling mode transitions from a capacitively coupled mode to an inductively coupled mode at 150 W of RF power, and another transition from an inductively coupled mode to a helicon mode at 900 W of RF power. The electron temperature and plasma density are both significantly increased in the inductive and helicon modes compared with the capacitive mode [14, 15], leading to a higher degree of ionization and likely a higher ion recirculation rate, which is thought to be the reason for the increase in hydrogen production and the larger degree of methane decomposition at higher RF power. The 8 SCCM data in figure 4 also indicate this effect, and a methane decomposition percentage of up to $99.99 \pm 0.06\%$ is possible when the HPRC is operating in a helicon mode. However, the increased degree of decomposition comes at the expense of hydrogen production energy efficiency, as indicated by figures 5 and 6 where increased methane gas flow rates and increased RF power levels lead to higher energy costs for hydrogen production.

The HPRC does not seem to exhibit a saturation of hydrogen production with increasing gas flow rate, at least up to 18 SCCM (figure 5), and in fact the reaction becomes more energy efficient with increasing flow rate up to 20 SCCM at a given RF power level. This finding indicates that the electron temperature may have been higher than needed, and increasing the input methane flow rate serves to increase the throughput and production of hydrogen gas at the expense of a decrease in the electron temperature, at least for a fixed RF power level.

The most efficient hydrogen production occurs when the HPRC is in a capacitive mode at 100 W of RF power with a methane flow rate of 18 SCCM (figure 6). The HPRC is also nearly an order of magnitude more efficient at producing hydrogen with an input methane flow rate of 18 SCCM compared with 8 SCCM, indicating that a much higher methane throughput is possible, and in fact may be required in order to take advantage of the higher electron temperatures and higher plasma densities of inductive mode and helicon mode operation. Steady-state helicon plasma

source operation of up to 40 kW has been demonstrated with other devices, and even higher power levels are feasible [17], which is promising for increasing the total throughput and efficiency of a portable, commercial-grade HPRC with possible applications such as a vehicle refueling station.

4.1. The roles of the electron and ion sheaths

The advantage of the HPRC over previous plasma-based reformation techniques is the fact that ions are unable to escape the reaction chamber of the HPRC. Only electrons and neutrals can penetrate the strong electron sheath at the exit to the system [8, 14, 15]. In order to maintain quasineutrality during steady-state operation, the amount of electron loss from the plasma must be balanced by an equal amount of ion loss [18]. Neglecting secondary emission from ion–wall collisions, which is predicted to be small, electrons and ions are born at an equal rate within the RF discharge and an efficient loss mechanism for the ions must be realized in order to extract an equal amount of electron current from the plasma source. Although the HPRC was originally designed and optimized for electron production and extraction, it is the same process and utilization of the electron and ion sheaths that make the HPRC well suited for producing high-purity hydrogen from methane. Ultimately, plasma density and particle losses present the limiting factors for the total amount of methane that can be decomposed by the HPRC. It was previously demonstrated [14] that an electron sheath is responsible for the extraction of all random incident electron flux through an extraction aperture during total nonambipolar particle flow. In order to have total nonambipolar flow, the ratio of the allowable ion loss area to electron loss area must be [14]

$$\frac{A_\mathrm{i}}{A_\mathrm{e}} \approx \sqrt{\frac{2m_\mathrm{i}}{\pi m_\mathrm{e}}}, \tag{3}$$

where A_e is the electron loss area, A_i is the ion loss area, m_e is the electron mass and m_i is the ion mass. Similar to the electron sheaths within a dc plasma, the electron sheath within the HPRC exhibits a presheath, where the potential changes by an order of $T_\mathrm{e}/2e$ from the bulk region to the electron sheath region, where T_e is the electron temperature in eV. Similar electron sheath structures with Ar and Xe plasmas are generated with the HPRC; however the sheath amplitude is approximately the ionization potential of the neutral gas. This result indicates that enhanced ionization within the sheath region limits the amplitude of the electron sheath to a value that is close to the gas species ionization potential [15].

The electron sheath exists as a roughly 2D lens shaped surface at the exit aperture of the HPRC, where the surface is normal to the local magnetic field lines The amplitude of the electron sheath can be controlled separately through the variation in bias potential of the ion collection cylinder. In this way, an ion recycle rate could be achieved that would best suit a particular methane decomposition rate and hydrogen production energy efficiency.

The graphite cylinder within the quartz tube of the HPRC is used both for serving as a Faraday shield for the RF, which keeps plasma potential fluctuations below 0.1 V peak-to-peak, and for providing an ion loss area as per equation (3). Hydrogen ions that impact the graphite cylinder are neutralized and simply migrate back into the volume of the reaction chamber. However, carbon ions that impact the graphite cylinder tend to be collected as solid graphite dust. The graphite Faraday shield plays a critical role in preventing carbon soot from building up on the interior of the dielectric (quartz) reaction chamber, which would stop RF fields from penetrating the dielectric reaction chamber altogether.

4.2. Comparisons with steam–methane reformation

The HPRC in its present proof-of-concept form requires at least 3700 MJ for each kg of H_2 produced. Based on the trends in the data presented, further efficiency gains are expected from operation at higher RF power levels. The HPRC energy cost compares with an energy cost of approximately 13 MJ kg^{-1} H_2 for catalytic steam oxidation, and 100 MJ kg^{-1} H_2 for partial steam oxidation methods, though these energy costs do not include the energy required to sequester the emitted CO_2 [2]. There are several advantages over the current industrial-scale steam–methane reformation methods. Specifically, the HPRC inherently sequesters all of the carbon from the methane gas into solid graphite, and does not release CO_2, or other emissions, as a byproduct of the production of hydrogen gas, which can be an energy-intensive process to sequester. Additionally, the HPRC is a table-top sized device, which could allow for widespread distribution of local hydrogen production, with only the need of an input gas containing hydrogen (e.g., nonpotable water) and an electrical energy source. No large investment in an entire factory-scale device is needed and widespread distribution of hydrogen production devices may be a desirable attribute during the early stages of adoption within a larger network of vehicle refueling stations [2].

4.3. Comparisons with other plasma devices used to produce hydrogen

Plasma reformation of hydrocarbons has been attempted before and in most cases has been adopted as a catalytic stage within the more traditional steam–methane reformation methods [2–7]. These plasma reformers have typically employed an arc source, where a large electrical current is used to ionize a flowing stream of gas into a plasma that ends up having a low ionization fraction. In these devices, a traditional mix of methane and water vapor (or oxygen) is introduced into the arc source, where the electrical energy is transferred to the thermal energy of the input gases, raising the temperature of the input gases to between 2000 and 3000 K [2]. While arc sources, in principle, are relatively simple devices and can handle large power densities, they are limited in their ability to produce high ionization fractions. Helicon plasma sources, on the other hand, are known to be one of the most efficient devices for generating plasma [19], often producing plasma densities exceeding 10^{14} cm^{-3} [17], and couple the majority of the input energy directly to the electrons instead of the ions, forming a low temperature nonthermal plasma with ion temperatures of

approximately 1200 K or less [14]. A nonthermal plasma is attractive because of the promise of coupling more of the input energy to molecular dissociation instead of heating of the bulk input gas or ions. Furthermore, unlike arc sources that ionize only the propellant that passes through the narrow ionized filamentary arc structures, helicon sources are able to ionize the propellant within a large volume. Recently, helicon plasma sources have also been used to dissociate water vapor into hydrogen and oxygen gas with promising results [20]. Electron cyclotron resonance (ECR) plasma sources have also been used to decompose water vapor [21]. ECR hydrogen production is promising, though the relatively low plasma densities that are typical for these devices may make them ill-suited for larger hydrogen gas production rates. The work presented in this paper serves to illustrate the proof-of-concept use and efficacy of RF sources in a hydrogen production capacity, and further study is needed to fully optimize the HPRC and explore the full parameter space of RF power, input gas flow rate, electron temperature, plasma density and the possible use of water vapor or oxygen as a fraction of the input gas flow.

4.4. Molecular decomposition

Although this paper is limited in scope to a set of experiments performed using input methane gas, the molecular decomposition method employed here is applicable to a large variety of decomposition applications. The primary benefits of the HPRC are that solid carbon is collected on the graphite cylinder, and only hydrogen gas leaves the reactor, which should be true of any hydrocarbon containing only C and H. This process makes the device efficient because the CO, CO_2 and other gases do not need to be sequestered as is the case in steam reformation or other reforming techniques. Water vapor or other hydrogen-containing molecules would serve the same purpose as methane in the production of hydrogen gas. However, sequestering of other gas by-products (such as oxygen) would be required in the HPRC, as is necessary with other devices. Due to the very high degree of molecular decomposition demonstrated on methane ($99.99 \pm 0.06\%$), the HPRC device may also find application in the destruction of hazardous compounds into less complex species or their constituent elements, or in the creation of compounds or radicals that would normally be difficult to synthesize chemically because of large chemical potential barriers or unfavorable reaction kinetics.

5. Conclusion

The current method for hydrogen production involves dissociating hydrogen from hydrocarbons such as methane in a reaction with water vapor at very high temperatures. In such reactions, carbon dioxide gas and hydrogen gas are the resultant products. Currently, this process involves the production and emission of $\sim$0.3 mol CO_2 for 1 mol of H_2, resulting in large production of a greenhouse gas in the extraction of hydrogen from methane. The HPRC is a device that produces molecular hydrogen gas by the dissociation of hydrogen-rich compounds such as methane gas, CH_4. The resultant carbon is collected in the form of solid graphite at an ion collection stage and the hydrogen gas is pumped out of the chamber in the collection stage. A high-density RF helicon plasma source is used to generate a population of electrons that provides enough energy to dissociate and ionize the input methane gas into its constituent atoms and/or ions. The HPRC uses a Faraday shield with multiple axial slits in order to provide an ion loss area, while at the same time allowing the time-varying RF fields to penetrate the reaction chamber. It was determined that the Faraday shield plays a critical role in preventing carbon soot from building up on the interior of the dielectric reaction chamber. An electron sheath is utilized to provide a high recirculation rate of ions in order to ensure that the exiting neutral particles will have participated in a multitude of dissociation and ionization events. The ratio of the ion loss area (for ions traversing the ion sheath) to that of the exit aperture area (for electrons traversing the electron sheath) was carefully balanced so that the particle losses within the HPRC were in total nonambipolar flow, resulting in large recirculation rates of ions and consequently a very high degree of decomposition of the input methane. In one operating mode, greater than $99.99 \pm 0.06\%$ of the methane injected into the HPRC was decomposed into hydrogen gas and solid carbon. The HPRC in its present proof-of-concept form requires 37$\times$ more energy per kg of H_2 produced, compared with steam–methane reformation, though this energy comparison does not include the energy required to sequester the emitted CO_2 during the steam–methane reformation cycle. Based on the trends in the data presented, further efficiency gains are expected from operation at higher RF power densities and higher methane flow rates.

Acknowledgments

This work was supported by US Department of Energy Grants No DE-FG02-97ER54437. Support was also provided by the Wisconsin Space Grant Consortium for BL, formerly a University of Wisconsin-Madison graduate student.

References

[1] Ogden J 2001 Review of small stationary reformers for hydrogen production *Consultant Report to the International Energy Agency*

[2] Deminsky M, Jivotov V, Potapkin B and Rusanov V 2002 Plasma-assisted production of hydrogen from hydrocarbons *Pure Appl. Chem.* **74** 413–8

[3] Czernichowski A 2001 Glidarc assisted preparation of the synthesis gas from natural and waste hydrocarbon gases *Oil Gas Sci. Technol. Rev. IFP* **56** 181–98

[4] Bromberg L, Cohn D, Rabinovich A and Alexeev N 1999 Plasma catalytic reforming of methane *Int. J. Hydrogen Energy* **24** 1131–7

[5] Sobacchi M, Saveliev A, Fridman A, Kennedy S A L A and Krause T 2002 Experimental assessment of a combined plasma/catalytic system for hydrogen production via partial oxidation of hydrocarbon fuels *Int. J Hydrogen Energy* **27** 635–42

[6] Petitpas G, Rollier J, Darmon A, Gonzalez-Aguilar J, Metkemeijer R and Fulcheri L 2007 A comparative study of non-thermal plasma assisted reforming technologies *Int. J. Hydrogen Energy* **32** 2848–67

[7] Chao Y, Huang C, Lee H and Chang M 2008 Hydrogen production via partial oxidation of methane with plasma-assisted catalysis *Int. J Hydrogen Energy* **33** 664–71
[8] Gutsol A, Rabinovich A and Fridman A 2011 Combustion-assisted plasma in fuel conversion *J. Phys. D: Appl. Phys.* **44** 274001
[9] Longmier B 2007 Plasma sheath behavior in a total nonambipolar radio frequency generated plasma electron source *PhD Thesis* University of Wisconsin–Madison
[10] Oleson S 2004 Electric propulsion technology development for the jupiter icy moons orbiter project *National Aeronautics and Space Administration Report No NASA/TM*-2006-214035
[11] Foster J and Patterson M 2005 Characterization of 40-centimeter microwave electron cyclotron resonance ion source and neutralizer *AIAA J. Propulsion Power* **21** 862–9
[12] Foster J, Williams G and Patterson M 2007 Characterization of an ion thruster neutralizer *AIAA J. Propulsion Power* **23** 828–35
[13] Chen F 1991 Plasma ionization by helicon waves *Plasma Phys. Control. Fusion* **33** 339
[14] Godyak A, Piejak R and Alexandrovich B 1995 The electron-energy distribution function in a shielded argon radiofrequency inductive discharge *Plasma Sources Sci. Technol.* **4** 332
[15] Longmier B and Hershkowitz N 2006 Nonambipolar electron source *Rev. Sci. Instrum.* **77** 113504
[16] Longmier B and Hershkowitz N 2008 Improved operation of the nonambipolar electron source *Rev. Sci. Instrum.* **79** 093506
[17] Severn G D and Hershkowitz N 1992 Radial control of the electrostatic potential in a tandem mirror with quadrupole end cells *Phys. Fluids* B **4** 3210
[18] Longmier B, Cassady L, Ballenger M, Carter M, Díaz F C, Glover T, Ilin A, McCaskill G, Olsen C and Squire J 2011 VX-200 magnetoplasma thruster performance results exceeding 50% thruster efficiency *AIAA J. Propulsion Power* **27** No 4
[19] Chen F 1995 *Proc. 37th Annual Meeting of the Division of Plasma Physics of the American Physical Society (Louisville, KY)*
[20] Boswell R and Chen F 1997 Helicons—the early years *IEEE Trans. Plasma Sci.* **25** 1229–44
[21] Nguyen S, Foster J and Gallimore A 2009 Operating a radio-frequency plasma source on water vapor *Rev. Sci. Instrum.* **80** 083503
[22] Givotov V, Fridman A, Krotov M, Krasheninnikov E and Patrushev B 1981 Plasmochemical methods of hydrogen production *Int. J. Hydrogen Energy* **6** 441–9